ELSEVIER

Journal of Alloys and Compounds 360 (2003) 98–106

Journal of ALLOYS AND COMPOUNDS

www.elsevier.com/locate/jallcom

Thermodynamic optimization of the lead-free solder system Bi–In–Sn–Zn

N. Moelans*, K.C. Hari Kumar, P. Wollants

Departement Metaalkunde en Toegepaste Materiaalkunde, K.U. Leuven, Kasteelpark Arenberg 44, 3001 Leuven, Belgium

Received 4 December 2002; received in revised form 11 February 2003; accepted 11 February 2003

Abstract

The Bi–In–Sn–Zn system is an important alloy system in lead-free soldering. Thermodynamic descriptions for the ternary systems Bi–In–Sn, Bi–In–Zn, Bi–Sn–Zn and In–Sn–Zn are optimized, using the CALPHAD method and combined to obtain a description of the quaternary Bi–In–Sn–Zn. All available experimental data from the literature are taken into consideration in the optimization. Calculated liquidi, isothermal and vertical sections and thermodynamic properties are compared with experimental data. Ternary and quaternary invariant reactions are also calculated.
© 2003 Elsevier B.V. All rights reserved.

Keywords: Alloys; Thermodynamic modelling; Phase diagram; Soldering

1. Introduction

The development of lead-free solder materials has received much attention in recent years. The principal reason for this is that the use of lead in microelectronics is being more and more restricted by legislation because of environmental and health concerns. Further, new lead-free solders can offer improved properties and extend the current range of application of the soldering technology. A candidate lead-free solder alloy must fulfil many requirements: wettability of the substrate, ability to form a strong chemical bond with the substrate, suitable melting temperature and solidification behavior, good mechanical properties like high strength and good resistance to mechanical and thermal fatigue, corrosion resistance, good electrical conductivity, safe for health and environment, possibility for easy assembly and low material cost. Phase diagrams can provide valuable information about the candidate solder alloys, like melting temperature and composition and fraction of the phases present in the microstructure.

The purpose of this article is to present a thermodynamic database for the Bi–In–Sn–Zn system, composed according to the CALPHAD method. Bi–In–Sn–Zn is an important system in lead-free soldering. Sn-rich Bi–In–Sn–Zn alloys are considered as substitutes for the near eutectic Pb–Sn alloys that are widely used in microelectronics. Experimental data [1–4] are promising: Bi–In–Sn–Zn alloys with high Sn-content are able to wet Cu-substrates, have a melting temperature which is close to that of the eutectic 37 wt.% Pb–63 wt.% Sn solder alloy, i.e. 183 °C, and offer better mechanical properties, in particular improved strength and resistance to creep. The thermodynamic database will be useful in the further development and optimization of lead-free Bi–In–Sn–Zn solder alloys.

2. Thermodynamic modelling

In the present study, the four ternary subsystems have been optimized using experimental data from the literature. Gibbs energy expressions of the elements have been taken from the SGTE database [5], as far as possible. Thermodynamic descriptions for the binary subsystems were optimized before [6–10], and have been used in the present work. Quaternary interactions have been neglected.

2.1. Phases

The following phases are considered: Liquid, Rhomb-A7, Tetr-A6, bct-A5, hcp-Zn, BiIn, Bi_3In_5, $BiIn_2$, β-A6 and InSn-γ. Detailed information about the phases is given in Table 1. The phases Rhomb-A7, Tetr-A6, bct-A5 and hcp-Zn correspond, in that order, to the stable states of Bi,

*Corresponding author.
E-mail address: nele.moelans@mtm.kuleuven.ac.be (N. Moelans).

0925-8388/03/$ – see front matter © 2003 Elsevier B.V. All rights reserved.
doi:10.1016/S0925-8388(03)00325-6

Table 1
Details of phases in the Bi–In–Sn–Zn system

Name	Pearson symbol	Constitution
Liquid, L		(Bi, In, Sn, Zn)
Rhombohedral-A7, (Bi)	hR2	(Bi, In, Sn, Zn)
Tetragonal-A6, (In)	tI2	(Bi, In, Sn, Zn)
bct-A5, (Sn)	tI4	(Bi, In, Sn, Zn)
hcp-Zn, (Zn)	hP2	(Bi, In, Sn, Zn)
BiIn	tP4	$(Bi)_{1/2}(In)_{1/2}$
Bi_3In_5	tI32	$(Bi)_{3/8}(In)_{5/8}$
$BiIn_2$	hP6	$(Bi)_{1/3}(In)_{2/3}$
β-A6, (β)	tI2	(Bi, In, Sn)
InSn-γ, (γ)	hP5	(In, Sn)

In, Sn and Zn, at a temperature of 25 °C and a pressure of 1 bar (denoted SER—Standard Element Reference). An explicit distinction is made between the hexagonal structure of Zn (hcp-Zn) and the ideal hexagonal close packed structure (hcp-A3) because the c/a-ratio (1.86) of Zn deviates considerably from the ideal c/a-ratio (1.63) of the hexagonal close packed structure. The diamond structure, which is the stable crystal structure of Sn below 13 °C, is not considered here.

In the In–Sn system [7], there are two intermediate phases with large homogeneity range. These are designated as InSn-β and InSn-γ. The Bi–In system [6] has four intermediate phases. BiIn, Bi_3In_5 and $BiIn_2$ are stoichiometric phases. The fourth phase, BiIn-ε, has a large homogeneity range. In fact both InSn-β and BiIn-ε have a tetragonal structure and their c/a-ratio is very similar (respectively, 1.27 and 1.29). Hence they are treated as a single phase, denoted by β-A6. The room temperature phase of In (Tetr-A6), has a tetragonal structure with a c/a-ratio of 1.52, which is considerably different from that of the β-A6 structure. Thus a distinction between both phases is made.

There are no stable ternary or quaternary phases known in the Bi–In–Sn–Zn system.

2.2. Gibbs energy models

In general, the Gibbs energy functions for the elements are accepted from the SGTE-database [5], taking into consideration updates until 1999 [11]. However if the necessary Gibbs energy functions are not available in the SGTE database, or if there are well founded reasons to do so, a different function than recommended by the SGTE database is used. Table 2 lists the Gibbs energy functions for elements that differ from Ref. [5] and are used in the present work. For Bi, In, and Sn ${}^\circ G_i^{\text{hcp-Zn}}$ is approximated from corresponding functions for hcp-A3, by adding +1 J/mol to ${}^\circ G_i^{\text{hcp-A3}}$. For Zn, Ref. [11] suggests:

$$\begin{aligned}\text{GHSERZN} = {} & -7285.787 + 118.470069\cdot T \\ & - 23.701314\cdot T\cdot \ln T \\ & - 1.712034\times 10^{-3}\cdot T^2 \\ & - 1.264963\times 10^{-6}\cdot T^3; \\ 298 < T < 692.68\ \text{K} = {} & -11\,070.559 \\ & + 172.34566\cdot T \\ & - 31.38\cdot T\cdot \ln T \\ & + 470.514\times 10^{24}\cdot T^{-9}; \\ 692.68 \le T < 1700\ \text{K}\end{aligned}$$

where $\text{GHSERZN} = {}^\circ G_{\text{Zn}}^{\text{hcp-Zn}} - {}^\circ H_{\text{Zn}}^{298}$ is expressed in J/mol. To reflect these changes, it was necessary to modify the binary descriptions of In–Sn [7] and Sn–Zn [10] (see Section 4.1).

Table 2
Updated Gibbs energy functions for elements

Quantity (J/mol)	Reference
${}^\circ G_{\text{Bi}}^{\text{β-A6}} - {}^\circ G_{\text{Bi}}^{\text{Rhomb-A7}} = +4234$	[11]
${}^\circ G_{\text{Bi}}^{\text{bct-A5}} - {}^\circ G_{\text{Bi}}^{\text{Rhomb-A7}} = +13\,526.3$	[7]
${}^\circ G_{\text{In}}^{\text{bct-A5}} - {}^\circ G_{\text{In}}^{\text{Tetr-A6}} = +2092$	[7]
${}^\circ G_{\text{In}}^{\text{Rhomb-A7}} - {}^\circ G_{\text{In}}^{\text{Tetr-A6}} = +4184$	[11]
${}^\circ G_{\text{In}}^{\text{β-A6}} - {}^\circ G_{\text{In}}^{\text{Tetr-A6}} = -33 + 0.16\cdot T$	[6]
${}^\circ G_{\text{In}}^{\text{hcp-Zn}} - {}^\circ G_{\text{In}}^{\text{Tetr-A6}} = +534 - 0.6868\cdot T$	[11]
${}^\circ G_{\text{Sn}}^{\text{Tetr-A6}} - {}^\circ G_{\text{Sn}}^{\text{bct-A5}} = +5387.0 - 8.26212\cdot T$	[7]
${}^\circ G_{\text{Sn}}^{\text{hcp-Zn}} - {}^\circ G_{\text{Sn}}^{\text{bct-A5}} = +3901 - 7.646\cdot T$	[11]
${}^\circ G_{\text{Sn}}^{\text{β-A6}} - {}^\circ G_{\text{Sn}}^{\text{bct-A5}} = +5015.5 - 7.5\cdot T$	[7]
${}^\circ G_{\text{Zn}}^{\text{Rhomb-A7}} - {}^\circ G_{\text{Zn}}^{\text{hcp-Zn}} = +2300 + 11.5\cdot T$	[11]
${}^\circ G_{\text{Zn}}^{\text{hcp-A3}} - {}^\circ G_{\text{Zn}}^{\text{hcp-Zn}} = +2969.82 - 1.56968\cdot T$	[11]

Liquid, the terminal phases (Rhomb-A7, Tetr-A6, bct-A5, hcp-Zn), β-A6 and InSn-γ are modelled using a random substitutional solution. The composition dependence of the Gibbs energy of these phases in the quaternary system can then be approximated from the Gibbs energies of the subsystems using the Muggianu extrapolation formula [12]:

$$G = \sum_i x_i\,{}^\circ G_i + RT\sum_i x_i \ln(x_i) + \sum_i\sum_{j\neq i} x_i x_j L_{i,j} + \sum_i\sum_{j\neq i}\sum_{k\neq j} x_i x_j x_k L_{i,j,k} \quad (1)$$

where ${}^\circ G_i$ is the Gibbs energy of the pure component i in the same state as the concerned phase, x_i the mol fraction of component i, and $L_{i,j}$ a temperature and composition dependent binary interaction term [13]. The ternary interaction term $L_{i,j,k}$ has the following composition dependence:

$$L_{i,j,k} = x_i L_i + x_j L_j + x_k L_k \quad (2)$$

where the parameters L_i, L_j and L_k may have a temperature dependence.

The Gibbs energy of the stoichiometric phases is expressed as

$${}^\circ G_{\text{Bi}_p\text{In}_q} = p\cdot {}^\circ G_{\text{Bi}}^{\text{SER}} + q\cdot {}^\circ G_{\text{In}}^{\text{SER}} + a + b\cdot T \quad (3)$$

Table 3
Experimental constitutional data for the Bi–In–Sn system

Reference	Experimental technique	Range
[18]	Thermal analysis, LOM, XRD	BiIn–Sn section
[14]	Thermal analysis, LOM, XRD	$BiIn_2$–Sn section
[16]	Thermal analysis	Subsystem BiIn–In–Sn
[17]	LOM, SEM, XRD	Eutectic with composition 31.6 wt.% Bi, 48.8 wt.% In, 20.6 wt.% Sn
[15]	Thermal analysis, LOM, SEM, XRD	Near $BiIn_2$–Sn section
[19]	Thermal analysis LOM, XRD	Subsystem Bi–BiIn–Sn
[20]	LOM, SEM	Near eutectic with composition 57.2 wt.% Bi, 24.8 wt.% In, 18 wt.% Sn
[21]	Thermal analysis, XRD, EDX	Entire system

where p and q are stoichiometric numbers and a and $-b$ are the enthalpy and entropy contribution to the Gibbs energy of Bi_pIn_q.

The last column in Table 1 shows the constituents of the various phases. Note that all four components are present only in the liquid phase and in the terminal phases.

3. Experimental data

The optimization of the ternary subsystems is based on constitutional and thermochemical data that can be found in the literature. The available experimental information is discussed below and a review is given in Tables 3–6.

3.1. Bi–In–Sn

The section $BiIn_2$–Sn was determined in Ref. [14] using thermal analysis, X-ray diffraction (XRD) and microscopic analysis. Three phase regions are reported, hence the $BiIn_2$–Sn section is not quasibinary. On the other hand, thermal and metallographic analyses of a series of samples having compositions near the $BiIn_2$–Sn section in Ref. [15] suggest the section to be quasibinary.

A eutectic reaction at 59 °C, involving a liquid with the composition 31.6 wt.% Bi, 48.8 wt.% In and 19.6 wt.% Sn was reported in Ref. [16]. The microstructure of this eutectic alloy consists of 57 vol.% $BiIn_2$, 24 vol.% of an In-rich phase that was identified as the intermetallic InSn-β phase, and 19 vol.% of a Sn-rich phase that was identified as the InSn-γ phase [17].

The existence of two ternary invariant reactions near the $BiIn_2$–Sn section was proposed in Ref. [15]: a eutectic reaction, $L \rightleftharpoons Bi_3In_5 + BiIn_2 + \gamma$, at 56 °C and a peritectic reaction, $L + BiIn \rightleftharpoons Bi_3In_5 + \gamma$, at 46 °C.

The BiIn–Sn section was determined in Ref. [18] using thermal analysis, metallography and XRD. It was shown to be a quasibinary.

The subsystem Bi–BiIn–Sn was investigated in Ref. [19]. Thermal, metallographic and X-ray analyses were used. A ternary invariant reaction at 77.5 °C, including the liquid, a Sn-rich phase, a Bi-rich phase and the inter-

Table 4
Experimental thermochemical data for the Bi–In–Zn system

Reference	Experimental technique	Range
[22]	EMF	450–650 °C, 0–5 at.% In, 0–5 at.% Zn
[23]	Knudsen's effusion	352 °C, 0–30 at.% Zn

Table 5
Experimental data for the Bi–Sn–Zn system

Reference	Experimental technique	Range
Constitutional data		
[24]	Thermal analysis, LOM	Entire system
Thermochemical data		
[25]	EMF	450–550 °C, entire composition range
[26]	EMF	441–641 °C, entire composition range
[27]	EMF	427–627 °C, entire composition range
[22]	EMF	450–650 °C, 0–5 at.% Sn, 0–5 at.% Zn
[28]	EMF	450–650 °C, 0–5 at.% Bi, 0–5 at.% Zn
[29]	EMF	500 °C, 0–10 at.% Zn
[23]	Knudsen's effusion	352 °C, 0–30 at.% Zn

Table 6
Experimental data for the In–Sn–Zn system

Reference	Experimental technique	Range
Constitutional data		
[30]	Thermal analysis	Entire system
[31]	Thermal analysis, XRD	Entire system
[32]	Thermal analysis	Entire system
Thermochemical data		
[33]	EMF	441–532 °C, 0–10 at.% Sn, 0–10 at.% Zn
[34]	EMF	441–532 °C, 3 at.% Zn
[35]	EMF	420–550 °C, entire composition range
[23]	Knudsen's effusion	352 °C, 0–30 at.% Zn
[37]	Calorimetric measurement	494 °C and 634 °C, entire composition range
[36]	Calorimetric measurement	447 °C and 483 °C, entire composition range

metallic phase BiIn, was found. The eutectic liquid contained 18 wt.% Sn, 12 wt.% Bi and 70 wt.% BiIn. The solid solubilities at the Bi and BiIn ends were found to be negligible and the Sn-rich solid solution contained 55 wt.% Sn, 14 wt.% Bi and 31 wt.% BiIn at the eutectic temperature. According to Ref. [19], the system Bi–BiIn–Sn is an independent subsystem. From this presumption, the authors concluded that the invariant reaction must be eutectic because there are no more invariant reactions involving the liquid at a lower temperature in the Bi–BiIn–Sn system. SEM and EDX studies of the microstructure of the alloy with eutectic composition, carried out in Ref. [20], showed that the Sn-rich solid solution, involved in the eutectic reaction, has the same structure as the Sn-rich intermetallic phase InSn-γ. More recent results [21] reveal that the Sn-based solid solution in the eutectic structure has the bct structure of Sn (that is bct-A5), thus contradicting the findings of Ref. [20]. In the research in Ref. [21], the XRD-technique, which can distinguish crystal structures, was used to characterize the phases, while in Ref. [20], SEM and EDX, that can only determine the composition of the phases, were used. Thus the observations of Ref. [21] are considered to be more reliable, since the bct-A5 phase can dissolve a significant amount of In and it may be difficult to distinguish it from the InSn-γ phase by composition alone.

Theoretical calculations in Ref. [21] indicate that the systems BiIn–Sn and $BiIn_2$–Sn are not quasibinary and that the Bi–BiIn–Sn system is not independent. The calculations also reveal that the invariant reaction in the Bi–BiIn–Sn subsystem is peritectic, unlike asserted in Ref. [19] and that the other calculated invariant reactions do not correspond exactly to what was claimed in Refs. [14–17].

There is no experimental thermochemical information available for this system.

3.2. Bi–In–Zn

For this system, not much experimental information could be found. EMF-measurements at temperatures between 450 and 650 °C were carried out in Ref. [22]. Vapor pressures of Zn at 352 °C for several ternary alloys with a composition of Zn in the range from 0 to 30 at.% were measured in Ref. [23], using Knudsen's effusion method. No constitutional data are reported in the literature.

3.3. Bi–Sn–Zn

The influence of Sn on the liquid miscibility gap in the Bi–Zn system was investigated in Ref. [24] using thermal analysis. The data for the monovariant points, where both liquids and a Zn-rich solid phase are in equilibrium, are questionable, since an accurate measurement of the thermal arrests of alloys with compositions in and near the miscibility gap is difficult. In addition, it was assumed in Ref. [24] that the miscibility gap is symmetrical which is not necessarily true. The other data seem to be reliable.

The thermochemical properties were determined from EMF-measurements by various authors [22,25–29]. These measurements cover the temperature range between 450 and 650 °C. Vapor pressures of Zn at 352 °C were determined in Ref. [23] for alloys with a composition of Zn between 0 and 30 at.%.

3.4. In–Sn–Zn

Thermal analysis was carried out for alloys covering the entire In–Sn–Zn composition range: according to Ref. [30], there is a eutectic reaction at 106 °C; according to Ref. [31], this eutectic reaction occurs at 109 °C. The monovariant lines of the liquidus were determined in Ref. [32], also using thermal analysis.

Activities of Zn were obtained by several authors [33–35], using the EMF-technique. The measurements were carried out at temperatures between 420 and 550 °C. Vapor pressures of Zn at 352 °C for In–Sn–Zn alloys were also measured in Ref. [23]. Furthermore, some data for mixing enthalpies at temperatures between 440 and 640 °C are available from calorimetric measurements in Refs. [36,37].

Some of these experiments were carried out quite recently within the scope of the development of lead-free soldering alloys.

3.5. Bi–In–Sn–Zn

Only limited information about the quaternary system is available. Some Sn-rich alloys were analyzed by differential scanning calorimetry [4]. The microstructure was examined using SEM and XRD.

4. Optimization

The thermodynamic descriptions of the binaries are from previous optimizations [6–10], with some modifications in the case of In–Sn and Sn–Zn, as described below. The ternaries have been optimized using the PARROT-module of the Thermo-Calc databank system [38]. Since the available experimental information about the solid phases is very limited and the properties of the liquid are of major importance in soldering, only the liquid has been considered in the optimization of the ternaries. All thermodynamic parameters that have been obtained in this work are listed in Table 7.

4.1. Binaries

The description for β-A6 (InSn-β) in In–Sn has been reoptimized, because in the present work a different Gibbs energy expression for In in β-A6 than that used in Ref. [7]

Table 7
Thermodynamic parameters for the Bi–In–Sn–Zn system obtained in this work

	${}^{0}L^{\text{Tetr-A6}}_{\text{In,Sn}} = +718 - 1.495 \cdot T$
${}^{0}L^{\text{Liq}}_{\text{Bi,In,Sn}} = -1016$	${}^{1}L^{\text{Tetr-A6}}_{\text{In,Sn}} = -2217$
${}^{1}L^{\text{Liq}}_{\text{Bi,In,Sn}} = +15\,234$	${}^{0}L^{\text{Tetr-A6}}_{\text{Sn,Zn}} = +2500^{a}$
${}^{2}L^{\text{Liq}}_{\text{Bi,In,Sn}} = +6051$	${}^{0}L^{\text{Tetr-A6}}_{\text{Bi,In,Sn}} = +12\,000^{b}$
${}^{0}L^{\text{Liq}}_{\text{Bi,In,Zn}} = +13\,972$	
${}^{1}L^{\text{Liq}}_{\text{Bi,In,Zn}} = -18\,397$	${}^{0}L^{\text{bct-A5}}_{\text{In,Zn}} = +3500^{a}$
${}^{2}L^{\text{Liq}}_{\text{Bi,In,Zn}} = -20\,702$	${}^{0}L^{\text{bct-A5}}_{\text{Bi,In,Sn}} = -20\,000^{b}$
${}^{0}L^{\text{Liq}}_{\text{Bi,Sn,Zn}} = -14\,284 + 10.721 \cdot T$	
${}^{0}L^{\text{Liq}}_{\text{In,Sn,Zn}} = -3040$	${}^{0}L^{\text{hcp-Zn}}_{\text{In,Sn}} = +500^{a}$
${}^{1}L^{\text{Liq}}_{\text{In,Sn,Zn}} = -3053$	${}^{0}L^{\text{hcp-Zn}}_{\text{Sn,Zn}} = +29\,725$
${}^{2}L^{\text{Liq}}_{\text{In,Sn,Zn}} = -12\,299$	
	${}^{0}L^{\beta\text{-A6}}_{\text{Bi,Sn}} = +10\,000^{b}$
	${}^{0}L^{\beta\text{-A6}}_{\text{In,Sn}} = 35.7 - 4.561 \cdot T$

[a] The parameter value has been selected to avoid the phase becoming stable in the binary system concerned.
[b] The parameter has been introduced to allow the optimization of Bi–In–Sn.

has been chosen to make it compatible with the description for Bi–In found in Ref. [6].

For the Sn–Zn system, the description from Ref. [10] has been preferred to the descriptions from Refs. [9,39], as it takes into account the temperature dependence of the mixing enthalpy of the liquid. This temperature dependence was observed in Refs. [40,41]. The description for the hcp-Zn phase has been reoptimized, since the optimization in Ref. [10] is based on Gibbs energy functions for Sn and Zn in the hcp-Zn structure from Ref. [5] that were updated afterwards [11].

The parameters ${}^{0}L^{\text{hcp-Zn}}_{\text{Sn,Zn}}$, ${}^{0}L^{\beta\text{-A6}}_{\text{In,Sn}}$ and ${}^{1}L^{\beta\text{-A6}}_{\text{In,Sn}}$ have been chosen such that the invariant reactions are reproduced exactly as in the case of Refs. [7,10].

Some positive binary interaction parameters have been introduced to restrict the stability range of certain phases. Such parameters are marked ([a]) in Table 7.

4.2. Ternaries

To allow the optimization of the liquid in the Bi–In–Sn system, three extra parameters have been introduced. In Table 7 these parameters are marked ([b]). In the absence of experimental information, the value of the parameters for the Tetr-A6 phase and the β-A6 phase have been chosen so that the stability range of these phases is acceptable and the liquid could be optimized properly. The parameter for the bct-A5 phase has been determined by comparing calculated sections with some experimental data for the phase boundaries of bct-A5 that could be derived from Ref. [19].

During the optimization of the Bi–In–Zn liquid, it was necessary to watch that the values of the parameters evolved in such a way that they reproduce a miscibility gap with a plausible shape.

5. Discussion

The calculated systems have been compared with all the available experimental information. Differences between calculated and experimental values are justified and some striking findings are discussed.

5.1. Bi–In–Sn

The calculated liquidus and the liquidus as proposed in Refs. [15–17,20] are shown in the Figs. 1 and 2. Calculated temperatures and compositions of invariant reactions approach the experimental values from Refs. [15–17,20], but the type of the reactions, and the involved phases, can differ. For example, the invariant reaction in the Bi–BiIn–Sn subsystem is peritectic, unlike asserted in Refs. [19,20] and involves the bct-A5 phase instead of the InSn-γ phase, as is explained in Section 3.1. Information about the calculated and experimentally determined invariant reactions for the ternary systems is given in Table 8.

The calculated BiIn–Sn and $BiIn_2$–Sn sections are not quasibinary, but the calculated phase boundaries agree well with the experimentally determined points. There is a good agreement with the data of Ref. [21], except near the In corner. There, it was not possible to match the experimental points with a reasonable amount of parameters. More experimental data are necessary to determine the extra parameter ${}^{0}L^{\text{Tetr-A6}}_{\text{Bi,In,Sn}}$ properly and to obtain a better descrip-

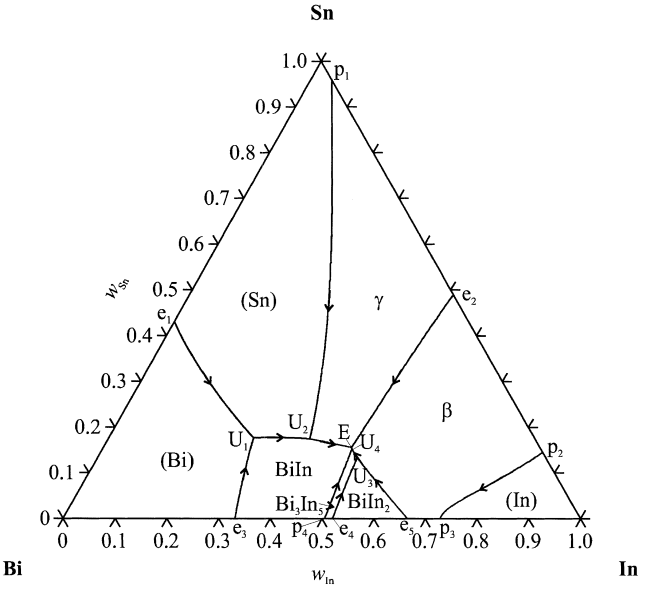

Fig. 1. Calculated liquidus of the Bi–In–Sn system.

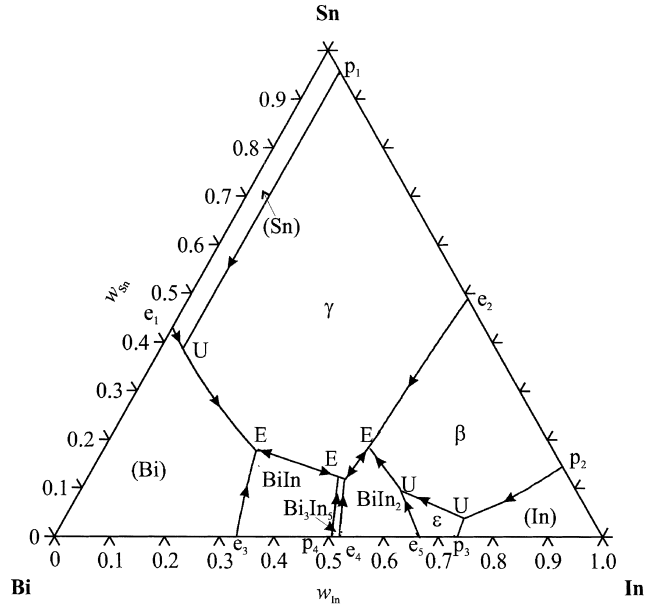

Fig. 2. Liquidus of the Bi–In–Sn system according to Refs. [15–17,20].

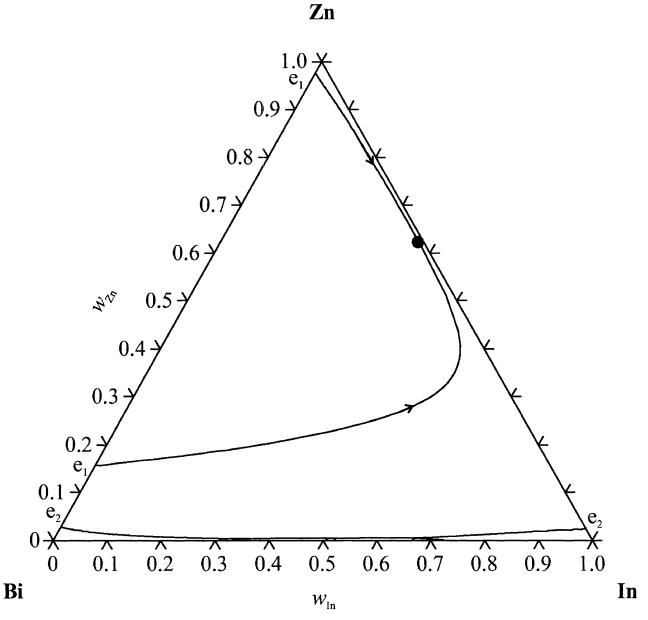

Fig. 3. Calculated liquidus of the Bi–In–Zn system.

tion of the system in this composition range. The experimental data from Ref. [19] are very well reproduced.

5.2. Bi–In–Zn

In Fig. 3, the calculated liquidus is shown. In order to make the nature and relative position of the invariant reactions visible, an enlarged representation of the region near the Bi–In side is given in Fig. 4. The calculated activities of Zn match very well the experimental values.

It is evident that additional experimental information will make the optimization more reliable. Nevertheless, this optimization provides valuable indications about phase stabilities, the existence and position of invariant reactions and the evolution of thermodynamic properties throughout the Bi–In–Zn system.

Table 8
Calculated and experimentally observed invariant reactions for the systems Bi–In–Sn, Bi–In–Zn, Bi–Sn–Zn and In–Sn–Zn

System	Reaction	Type	t (°C)	Composition of the liquid (wt.%)				Reference
				Bi	In	Sn	Zn	
Bi–In–Sn	$L \rightleftharpoons (Bi)+(Sn)+BiIn$	E	77.5	57.2	24.8	18.6		[19]
	$L+(Bi) \rightleftharpoons (Sn)+BiIn$	U_1	75.22	54.3	27.9	17.7		[a]
	$L+(Sn) \rightleftharpoons BiIn+\gamma$	U_2	70.38	43.2	39.3	17.5		[a]
	$L+BiIn \rightleftharpoons Bi_3In_5+\gamma$	U	64					[15]
	$L+BiIn_2 \rightleftharpoons Bi_3In_5+\beta$	U_3	60.57	36.1	50.2	13.7		[a]
	$L \rightleftharpoons BiIn_2+\beta+\gamma$	E	59	31.6	48.8	19.6		[17]
	$L+Bi_3In_5 \rightleftharpoons BiIn+\beta$	U_4	58.99	36.1	48.3	15.5		[a]
	$L \rightleftharpoons BiIn+\beta+\gamma$	E_1	58.98	36.1	48.3	15.6		[a]
	$L \rightleftharpoons Bi_3In_5+BiIn_2+\gamma$	E	56.5					[15]
Bi–In–Zn	$L \rightleftharpoons (Bi)+(Zn)+BiIn$	E_1	107.86	66.3	33.4		0.3	[a]
	$L+BiIn \rightleftharpoons (Zn)+Bi_3In_5$	U_1	86.81	48.8	50.8		0.4	[a]
	$L \rightleftharpoons (Zn)+Bi_3In_5+BiIn_2$	E_2	85.78	47.4	52.2		0.4	[a]
	$L+\beta \rightleftharpoons (In)+BiIn_2$	U_2	67.86	32.7	66.9		0.4	[a]
	$L \rightleftharpoons (In)+(Zn)+BiIn_2$	E_3	67.77	32.7	66.9		0.5	[a]
Bi–Sn–Zn	$L \rightleftharpoons (Bi)+(Sn)+(Zn)$	E	131.24	53.7		44.2	2.1	[a]
	$L \rightleftharpoons (Bi)+(Sn)+(Zn)$	E	129.87	56		40	4	[24]
In–Sn–Zn	$L+(Sn) \rightleftharpoons (Zn)+\gamma$	U_1	183.29		10.1	83.8	6.2	[a]
	$L+(In) \rightleftharpoons (Zn)+\beta$	U_2	121.54		76.5	21.8	1.6	[a]
	$L \rightleftharpoons (Zn)+\beta+\gamma$	E	109					[31]
	$L \rightleftharpoons (Zn)+\beta+\gamma$	E	107.41		52.3	46.3	1.4	[a]
	$L \rightleftharpoons (Zn)+\beta+\gamma$	E	106.4					[30]

[a] Obtained in this work.

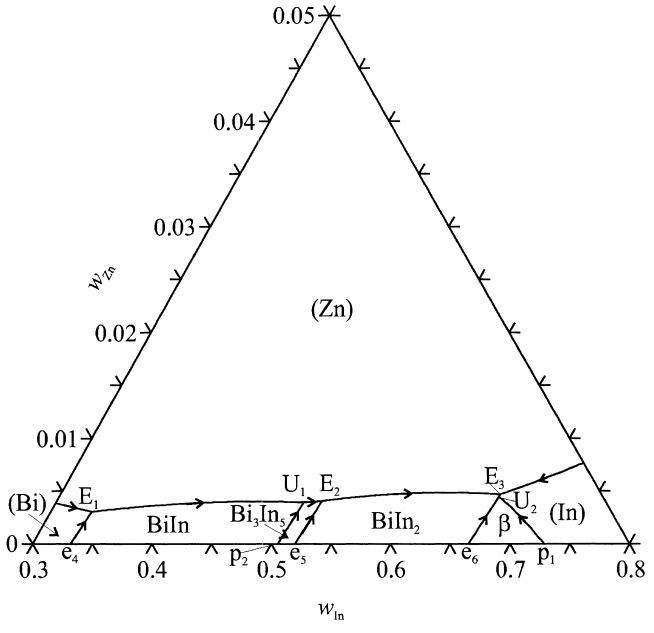

Fig. 4. Magnification of the liquidus of the Bi–In–Zn system near the Bi–In side.

5.3. Bi–Sn–Zn

The calculated liquidus is shown in Fig. 5. The experimental data for the monovariant points have been added. During the optimization of the Bi–Sn–Zn system, it turned out that the experimental data for points in and near the miscibility gap from Ref. [24] are indeed inconsistent with other data. This is also clear from Fig. 5. The miscibility gap is not symmetrical and the calculated tie-lines are not parallel to the Bi–Zn system. Except for the shape of the miscibility gap, the calculated liquidus matches very well the experimental points. The calculated temperature and composition of the eutectic are nearly the same as the experimental values (Table 8). The correspondence between calculated vertical sections and experimental data is also very good. Calculated thermochemical properties agree very well with the experimental values.

Although no experimental information about the miscibility gap is used in the optimization, it is probable that the position of the miscibility gap is accurately predicted. The optimization is based on sufficient, accurate and widely spread thermochemical data outside the miscibility gap, so that the optimized expressions for the Gibbs energy are also valid inside the miscibility gap.

The expression for the Bi–Sn–Zn system obtained in this work is less complicated than that obtained in Ref. [42], which is based on different descriptions for the Bi–Sn and Sn–Zn systems [39,43]. The straightforwardness of the present optimization can probably be attributed to a better choice of binary descriptions, especially Ref. [10] which contains a $T\ \ln(T)$-term.

5.4. In–Sn–Zn

In Fig. 6, the calculated liquidus, together with the experimental data for the monovariant points, is shown. The eutectic temperature is equal to 107.4 °C, which is in between the two experimental values. In the calculated diagram, there are also two peritectic reactions involving the liquid. From the presence of several invariant reactions in the In–Sn system, it can be expected that, indeed, there must be more than one invariant reaction in the ternary

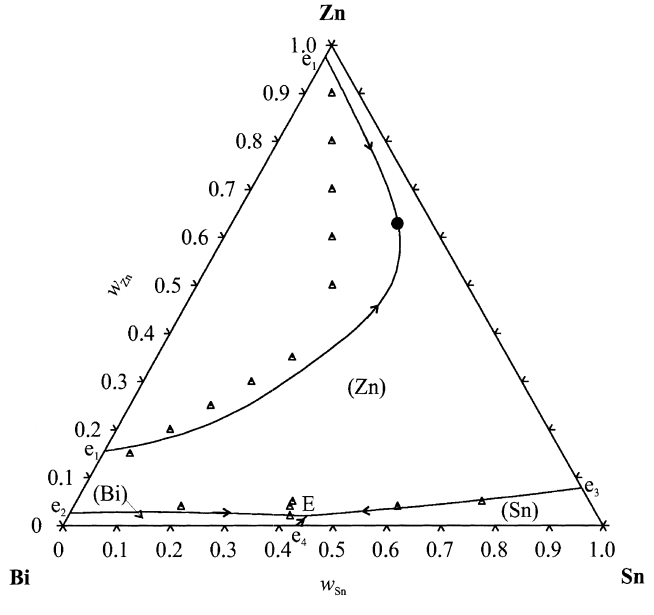

Fig. 5. Calculated liquidus of the Bi–Sn–Zn system. Experimental data from Ref. [24] are superimposed.

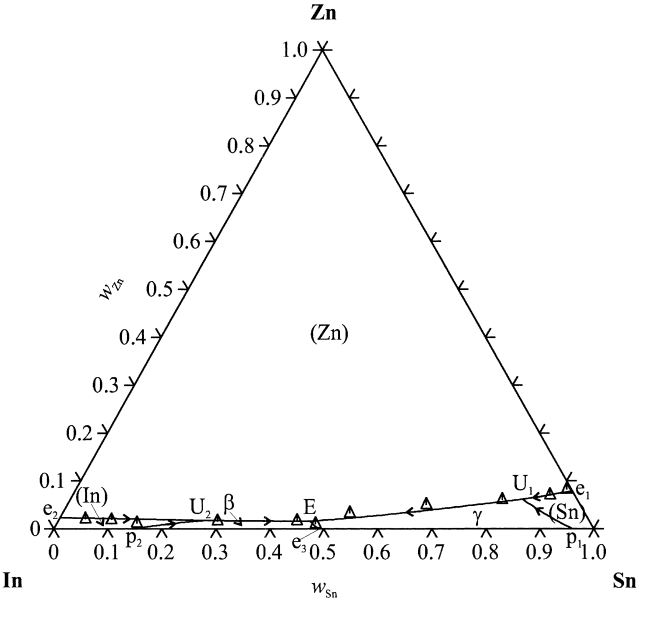

Fig. 6. Calculated liquidus of the In–Sn–Zn system. The experimental data from Ref. [32] are superimposed.

system, but those have never been observed experimentally.

Calculated sections agree very well with the experimental data from thermal analysis, except for one respect which is illustrated in Fig. 7. According to Ref. [30], there should occur a eutectic reaction in alloys with a composition that belongs to the section $x_{In}/x_{Sn} = \frac{15}{85}$. On the other hand, since the phase InSn-γ is modelled without solubility of Zn, the extent of the invariant triangle cannot be influenced by ternary interaction parameters. The angle of the invariant triangle representing the composition of InSn-γ belongs to the boundary system In–Sn. Its position is fixed once a description for the binaries is chosen. If the experimental data are correct, they suggest solubility of Zn in the InSn-γ phase, but the amount of data is too limited to model it. Moreover, in order to describe a solubility of Zn in InSn-γ, an expression for ${}^{\circ}G_{Zn}^{InSn\text{-}\gamma}$ should be composed.

Furthermore, it was not possible to model the correct temperature dependence of the mixing enthalpy. In some regions of the diagram, the calculated temperature dependence is opposite to what is experimentally observed (Fig. 8). In these regions, the experimentally determined mixing enthalpy increases with increasing temperature, whereas the calculated mixing enthalpy decreases with increasing temperature anywhere in the system. This negative temperature dependence in the calculated mixing enthalpy originates from the $T\ \ln(T)$-term used in the description for the Sn–Zn system. As mentioned in Section 4.1, this negative temperature dependence is present in the Sn–Zn system, but apparently the temperature dependence shifts in the ternary system. This change in temperature dependence could be modelled by including a $T\ \ln(T)$-term in the description of the ternary interaction parameters. But the available data cover too narrow a temperature and composition range and are not accurate enough.

Calculated activities agree well with the experimental data.

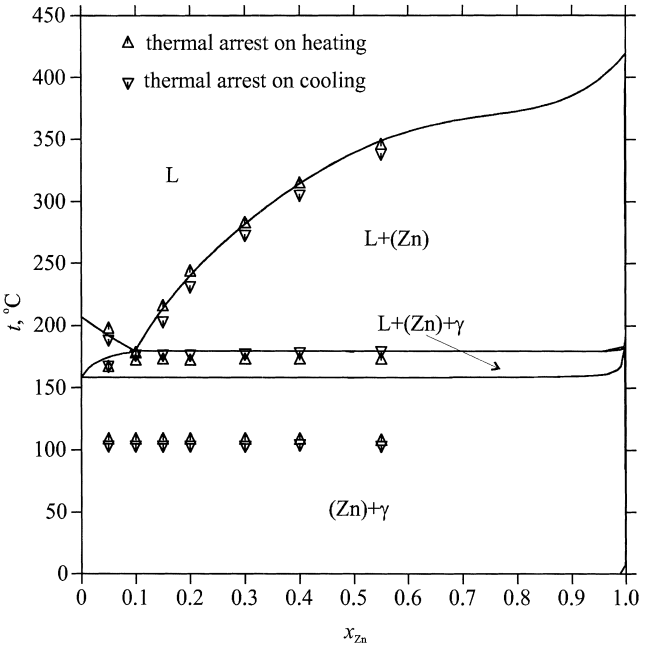

Fig. 7. Calculated vertical section of the In–Sn–Zn system for x_{In}/x_{Sn} = 15/85 compared with experimental data from Ref. [30].

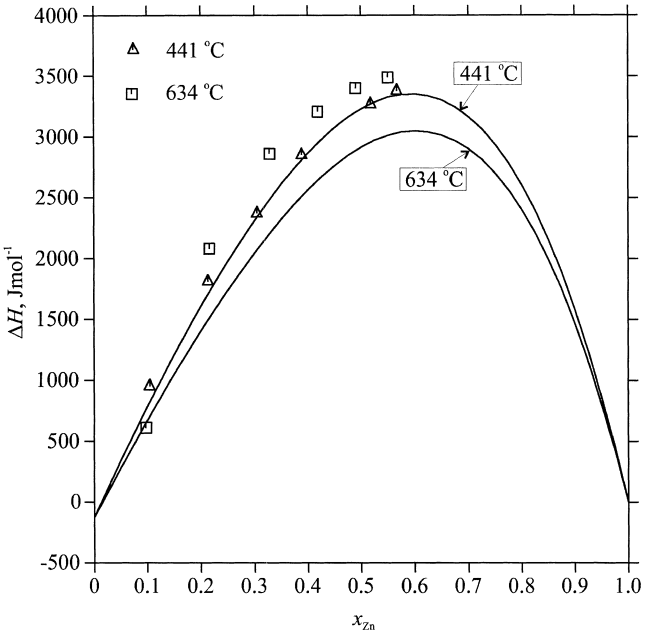

Fig. 8. Calculated mixing enthalpy at 441 and 634 °C for the section $x_{In}/x_{Sn} = 0.25/0.75$ of the In–Sn–Zn system, compared with experimental data from Ref. [37].

5.5. Bi–In–Sn–Zn

A thermodynamic dataset for the quaternary has been obtained by merging the descriptions of the subsystems. The correspondence with the experimental data is quite good.

The quaternary invariant reactions involving the liquid have been calculated using Pandat [44]. The results are given in Table 9. The lowest melting point of the system appears to be at 57.2 °C.

6. Conclusion

The four ternary boundary systems of the quaternary system Bi–In–Sn–Zn have been optimized using constitutional as well as thermochemical experimental data that were available in the literature. The calculated results agree very well with the experimental data. The derived thermodynamic description of the system can be very useful in the design of lead-free Bi–In–Sn–Zn solder alloys.

Table 9
Calculated invariant reactions of the quaternary Bi–In–Sn–Zn system

Reaction	Type	t (°C)	Composition of the liquid (wt.%)			
			Bi	In	Sn	Zn
$L+(Bi)\rightleftharpoons(Sn)+(Zn)+BiIn$	U_1	74.12	53.5	28.0	18.1	0.4
$L+(In)\rightleftharpoons(Zn)+BiIn_2+\beta$	U_2	67.53	33.1	64.1	2.4	0.5
$L+(Sn)\rightleftharpoons(Zn)+BiIn+\gamma$	U_3	66.86	40.6	41.3	17.6	0.5
$L+BiIn\rightleftharpoons Bi_3In_5+\beta+\gamma$	U_4	58.85	36.1	48.3	15.6	0.3
$L+BiIn_2\rightleftharpoons(Zn)+Bi_3In_5+\beta$	U_5	58.45	35.0	50.2	14.4	0.4
$L+BiIn\rightleftharpoons(Zn)+Bi_3In_5+\gamma$	U_6	57.45	35.3	48.3	15.9	0.4
$L\rightleftharpoons(Zn)+Bi_3In_5+\beta+\gamma$	E_1	57.23	35.0	48.6	15.9	0.4

References

[1] M. McCormack, S. Jin, H.S. Chen, D.A. Machusak, J. Electron. Mater. 23 (7) (1994) 687.
[2] M. McCormack, S. Jin, J. Electron. Mater. 23 (7) (1994) 635.
[3] W.Y. Yoon, J.R. Soh, B.-J. Lee, H.M. Lee, Alloy design of Sn–Zn–X (X = In, Bi) solder systems through phase equilibria calculations, in: R.K. Mahidhara, D.R. Frear, S.M.L. Sastry, K.L. Murty, P.K. Liaw, W. Winterbottom (Eds.), Design and Reliability of Solders and Solder Interconnections, The Minerals, Metals and Materials Society, 1997, pp. 121–128.
[4] W.Y. Yoon, J.R. Soh, H.M. Lee, B.-J. Lee, Acta Mater. 45 (3) (1997) 951.
[5] A.T. Dinsdale, Calphad 15 (4) (1991) 317.
[6] D. Boa, I. Ansara, Thermochim. Acta 314 (1998) 79.
[7] B.-J. Lee, C.-S. Oh, J.-H. Shim, J. Electron. Mater. 25 (1996) 983.
[8] D.V. Malakhov, Calphad 24 (2000) 1.
[9] B.-J. Lee, Calphad 20 (1996) 471.
[10] S. Fries, H.L. Lukas, System Sn–Zn, in: I. Ansara, A.T. Dinsdale, M.H. Rand (Eds.), COST 507, Thermochemical Database for Light Metal Alloys, Vol. 2, 1998, pp. 288–289.
[11] A.T Dinsdale, unpublished data, 1991–1999.
[12] Y.-M. Muggianu, M. Gambino, J.-P. Bros, J. Chim. Phys. 72 (1) (1975) 83.
[13] O. Redlich, A.T. Kister, Ind. Eng. Chem. Res. 40 (2) (1948) 345.
[14] S.I. Stel'makh, V.A. Tsimmergaki, I.A. Sheka, Prog. Sov. Chem. 38 (1972) 631.
[15] H. Kabassis, J.W. Rutter, W.C. Winegard, Mater. Sci. Technol. 2 (1986) 985.
[16] S.I. Stel'makh, V.A. Tsimmergaki, I.A. Sheka, Ukr. Khim. Zh. 38 (1972) 855.
[17] H. Kabassis, J.W. Rutter, W.C. Winegard, Metall. Trans. 15A (1984) 1515.
[18] G.J. Dooley, E.A. Peretti, J. Chem. Eng. Data 9 (1964) 90.
[19] L.R. Scherpereel, E.A. Peretti, J. Mater. Sci. 2 (1967) 256.
[20] M.A. Ruggiero, J.W. Rutter, Mater. Sci. Technol. 11 (1995) 136.
[21] S.W. Yoon, B.-S. Rho, F.M. Lee, B.-J. Lee, Met. Mater. Trans. 30A (1999) 1503.
[22] J.V. Gluck, R.D. Pehlke, Trans. AIME 239 (1967) 36.
[23] T. Yokokawa, A. Doi, K. Niwa, J. Phys. Chem. 65 (1961) 202.
[24] S.D. Muzaffar, J. Chem. Soc. 123 (1923) 2341.
[25] L. Oleari, M. Fiorani, Ric. Sci. 29 (1959) 2219.
[26] W. Ptak, M. Moser, Archiwum Hutnictwa 11 (1966) 289.
[27] C.W. Bale, A.D. Pelton, M. Rigaud, Z. Metallkd. 68 (1977) 69.
[28] R.L. Louvet, J.V. Gluck, R.D. Pehlke, Trans. AIME 242 (1968) 2369.
[29] V.N.S. Mathur, M.L. Kapoor, Z. Metallkd. 76 (1985) 16.
[30] A. Sabbar, A. Zrineh, M. Gambino, J.P. Bros, Thermochim. Acta 369 (2001) 125.
[31] Y. Xie, H. Schicketanz, A. Mikula, Ber. Bunsenges. Gesellsch. 102 (1998) 1334.
[32] Y. Zheng, Q. Zhang, Acta Phys. Chim. 14 (1998) 1098.
[33] Z. Moser, W. Szponder, Bull. Acad. Polon. Sci., Sér. Sci. Techn. 21 (1973) 705.
[34] Z. Moser, Z. Metallkd. 65 (1974) 106.
[35] Y. Nakamura, M. Shimoji, K. Niwa, Trans. Jpn. Inst. Met. 5 (1964) 28.
[36] J.M. Fiorani, C. Naguet, J. Hertz, A. Bourkba, L. Bouirden, Z. Metallkd. 88 (1977) 711.
[37] P. Anrés, M. Alaoui-Elbelghiti, M. Gambino, J.P. Bros, Thermochim. Acta 346 (2000) 49.
[38] B. Sundman, B. Jansson, J.-O. Andersson, Calphad 9 (1985) 153.
[39] H. Ohtani, M. Miyashita, K. Ishida, J. Jpn. Metal. 63 (1999) 685.
[40] O.J. Kleppa, J. Phys. Chem. 59 (1955) 354.
[41] A. Bourkba, J.M. Fiorani, C. Naguet, J. Hertz, Z. Metallkd. 10 (1996) 773.
[42] D.V. Malakhov, S.L. Liu, I. Ohnuma, K. Ishida, J. Phase Equil. 21 (2000) 514.
[43] H. Ohtani, K. Ishida, J. Electron. Mater. 23 (1994) 747.
[44] Y.A. Chang, CompuTherm LLC, University of Wisconsin—Madison.